applied sciences

MDPI

Communication

Investigation of the Beam Quality of a Compact Non-Chain Pulsed DF Laser with a Confocal Positive Branch Unstable Resonator

Laiming Zhang [1], Peng Ruan [2], Fei Chen [1], Chunlei Shao [1,*], Qikun Pan [1,*] and Jin Guo [1]

[1] State Key Laboratory of Laser Interaction with Matter, Changchun Institute of Optics, Fine Mechanics and Physics, Chinese Academy of Sciences, Changchun 130033, China
[2] College of Information Technology, Jilin Engineering Research Center of Optoelectronic Materials and Devices, Jilin Normal University, Siping 136000, China
* Correspondence: sclem@sina.com (C.S.); panqikun2005@163.com (Q.P.)

Abstract: The results of detailed studies on the beam quality of a non-chain pulsed electric discharged DF laser based on a compact inner cavity confocal positive branch unstable resonator were presented herein. The theoretical and experimental divergence angles for magnification M = 1.65, 1.85, 2.05, and 2.25 were calculated according to Fraunhofer diffraction and measured by the method of calibrated apertures. The smallest divergence of θ = 0.66 mrad was obtained with M = 2.25 in our experiment, which is 1.95 times the theoretical value. The corresponding far-field energy density at 10 km distance from the laser exit was 82.8 mJ/m^2. The beam quality and energy density were increased by 11 and 91 times, respectively, compared with a similar stable resonator in our lab.

Keywords: DF lasers; positive branch unstable resonator; divergence angle; diffraction limit magnification

Citation: Zhang, L.; Ruan, P.; Chen, F.; Shao, C.; Pan, Q.; Guo, J. Investigation of the Beam Quality of a Compact Non-Chain Pulsed DF Laser with a Confocal Positive Branch Unstable Resonator. *Appl. Sci.* **2023**, *13*, 3229. https://doi.org/10.3390/app13053229

Academic Editor: Edik U. Rafailov

Received: 6 February 2023
Revised: 27 February 2023
Accepted: 28 February 2023
Published: 2 March 2023

1. Introduction

In the past ten years, there has been a considerable number of studies performed investigating repetitively non-chain pulsed HF/DF lasers because of their advantages of high output power, special infrared output band, compact and simple structure, and safe operation [1–7]. These advantages make lasers of this type promising for applications in many fields such as spectroscopy, laser radar transmitters, laser ranging, atmospheric monitoring, military, etc. [8–14]. Besides, non-chain short-pulsed HF/DF lasers comprise an ideal pump source for novel Fe:ZnSe lasers, the fluorescent lifetimes of which are 360 ns at T = 292 K, and this process can expand the laser spectrum to 4–5 μm [15–18].

In the past few years, most studies have focused on the achievement of high radiation energies (powers), high electric efficiency, and repetition rates in non-chain HF/DF lasers. The radiation energy up to 325 J at the electric efficiency of 3.4% was achieved in an electric discharged non-chain DF laser by applying self-initiated volume discharge in a SF_6–D_2 gas mixture [19]. This energy was achieved with a discharge gap d = 27 cm and it is the highest energy for non-chain DF lasers reported so far. A further increase of the generation energy of HF (DF) non-chain lasers to 1 kJ can be achieved by increasing the separation d between electrodes and the transversal dimension of the cathode, but this has very high power supply requirements. In Ref. [20], after optimizing the mixture composition, specific input energy, and uniformity of electric field, the highest electrical efficiency of 6.4% reported until now for non-chain DF lasers with electric discharge was attained by Tarasenko, and the output energy was more than 1 J. In Ref. [21], a 1 kHz high-repetition-rate non-chain HF/DF laser with an average laser output power of up to 2.5 W in SF_6–D_2 gas mixture was achieved by Harris. A 2.2 kHz repetition rate atmospheric pressure HF/DF laser with an output power of 33 W and electrical efficiency of 1.6% was obtained by Velikanov; the electric discharge was matched by diluting helium in the working mixture to preserve the

discharge conditions [22]. Applying three electric-discharge laser modules of the same type, a non-chain DF laser with 400 W output power at a pulse repetition rate of 10 Hz was obtained after optimizing the cavity Q-factor, the composition, and the total pressure of the working mixture [23]. A closed-cycle, repetitively pulsed HF laser with an output power of 55 W at 100 Hz was presented by optimizing gas flow velocity, performing a small replenishment of the working gas, and applying a 3A molecular sieve in the discharge chamber [24].

Although energy (power) is an important indicator for evaluating a laser's performance, many applications for mid-infrared lasers require not only high energy strength in emission, but also good beam quality. Stable resonator HF/DF lasers can easily achieve high output power and are simple to install and adjust, but the far-field divergence angle is relatively large compared with unstable resonator lasers. When the laser is transmitted for a certain distance, the laser beam spreads rapidly and its energy density decreases significantly, which limits the long-distance applications of stable repetitively pulsed HF/DF lasers. In remote atmosphere ecological monitoring, the laser beam needs to travel a distance of more than 10 km to detect air contaminants such as gaseous hydrocarbons, HCl, N_2O, and SO_2, so compressing the beam divergence is essential. However, the beam quality of non-chain pulsed HF/DF lasers has not yet been investigated sufficiently thoroughly. There are only a few papers which briefly introduce the results of divergence measurements. In Ref. [25], a good HF laser beam quality with a far-field divergence angle of 1.7 times the diffraction limit was attained using the method of calibrated apertures on an unstable telescope cavity with a magnification of $M = 2$. In Ref. [26], a radiation divergence of $\theta_{0.5} = 0.29$ mrad (containing 50% encircled energy), which corresponds to four diffraction limits, was achieved using an unstable telescopic resonator with $M = 3$ on a self-sustained volume-discharged non-chain DF laser. The radiation divergence measurements were carried out by the method of a focal spot with application of a reflecting wedge. In Ref. [27], a stable HF laser beam was obtained by adopting a confocal positive branch resonator with a magnification of $M = 3.4$. However, due to the lack of relevant beam quality diagnostic equipment, they did not give achieve a far-field divergence angle of the unstable laser system.

The unstable resonators used in the abovementioned studies applied external cavity structures, with discharge chambers sealed by CaF_2/BaF_2 windows and cavity mirrors placed outside the chambers. This type of resonator has the disadvantages of long structure, being difficult to adjust, suffering additional energy loss, and incurring extra costs caused by CaF_2/BaF_2 windows. In this paper, a compact intra cavity resonator was used. The goal governing the practical long-distance applications of this laser is increasing the energy (average power) of laser radiation and beam quality. The current paper performed a detailed investigation on the beam quality of a compact close-cycle electric-discharged non-chain pulsed DF laser with a confocal positive branch resonator, and the aim was the compression of the divergence angle in a limited energy range.

2. Theoretical Calculation of the Laser Beam Divergence

Figure 1 shows a schematic cross-sectional view of a typical unstable resonator. The convex output mirror has a diameter D_1 and radius of curvature R_1; the concave reflecting mirror has a diameter D_2 and radius of curvature R_2. The radii of curvature are defined as positive for concave mirrors and negative for convex ones. The mirror separation L is the resonator length. There are two types of unstable resonators: positive-branch and negative-branch. For high-power DF lasers, negative-branch unstable resonators should be avoided because of their solid focus in the cavity. In this paper, we only considered a confocal positive-branch unstable resonator, which produces a collimated output beam. The structures of the confocal positive-branch unstable resonator used in this paper were designed according to Ref. [28]. Table 1 shows the detailed parameters of our resonator. The magnification M is from 1.65 to 2.25, the resonator length L and reflecting mirror diameter

D_2 are fixed with L = 2.113 m and D_2 = 5 cm, and C is the output coupling coefficient calculated by $1 - 1/M^2$.

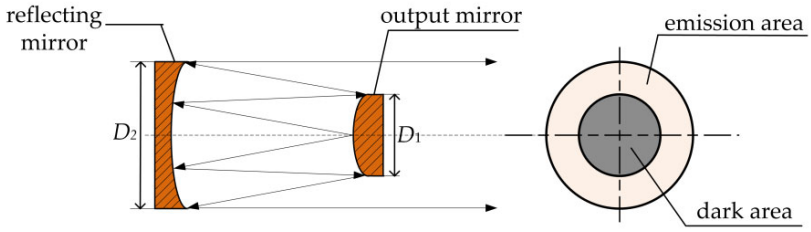

Figure 1. Structure of the positive-branch confocal unstable resonator.

Table 1. Structure parameters of the unstable resonator.

M	C	R_1/mm	R_2/mm	D_1/mm	D_2/mm	L/mm
1.65	0.633	−6501.5	10,727.5	30.2	50	2113
1.85	0.708	−4971.9	9197.8	26.9	50	2113
2.05	0.762	−4024.8	8250.8	24.2	50	2113
2.25	0.802	−3380.8	7606.8	22.2	50	2113

As we can see from Figure 1, for a strictly adjusted confocal positive branch resonator, the output beam can be seen as an ideal plane beam. The far-field distribution of the output laser can be given according to the Fraunhofer diffraction field distribution formed by the plane wave passing through the annular aperture [29]. The angular distribution of far-field intensity can be written as follows:

$$I(\theta) = \left\{ \frac{M^2}{(M^2-1)} \left[\frac{2J_1(ka\theta_s)}{ka\theta_s} - \frac{2J_1(ka\theta_s/M)}{Mka\theta_s} \right] \right\}^2 I_0 \quad (1)$$

where J_1 is the Bessel function of the first kind, θ_s is the semi-divergence angle, $k = 2\pi/\lambda$, a is the radius of reflecting mirror, and I_0 is the beam intensity at the center of the beam in far-field distribution. Let $Z = ka\theta$, and then expression (1) can be rewritten as follows:

$$I(Z) = \left\{ \frac{M^2}{(M^2-1)} \left[\frac{2J_1(Z)}{Z} - \frac{2J_1(Z/M)}{MZ} \right] \right\}^2 I_0 \quad (2)$$

The far-field relative energy distribution is as follows:

$$E(Z) = \int_0^Z \left\{ \frac{M^2}{(M^2-1)} \left[\frac{2J_1(Z)}{Z} - \frac{2J_1(Z/M)}{MZ} \right] \right\}^2 ZdZ \quad (3)$$

According to expressions (2) and (3), the far-field relative intensity and energy for different magnifications were plotted based on different Z values as shown in Figures 2 and 3.

Given the total energy of 100%, the energy proportion of the central main lobe for unstable resonator from M = 1.65 to 2.25 is 36.6%, 43.5%, 49.2%, and 53.8%, respectively. The larger the magnification, the higher the energy contained by the main lobe, meaning a better beam quality of the laser beam. As we can see from Figure 3, within the same divergence angle, the energy content of the far-field energy distribution of the unstable cavity with larger magnification M was bigger than that of the resonator with a small M. Therefore, with the gradual increase of M, the beam quality of the unstable resonator became better and better. Because circular laser beams usually have a Gaussian-shaped energy density distribution from the center of the beam to the edges, we used 86.5% encircled energy to definite the far-field spot size. Therefore, the far-field divergence angle can be calculated based on $\theta = 2Z/(ka)$. The calculated results for different magnifications with wavelength λ = 3.8 μm are shown in Table 2.

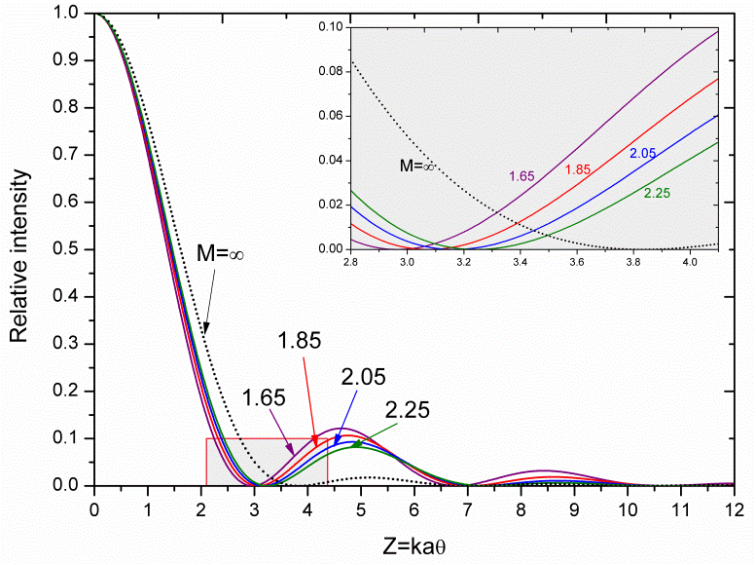

Figure 2. Relative intensity distribution versus Z under different magnifications.

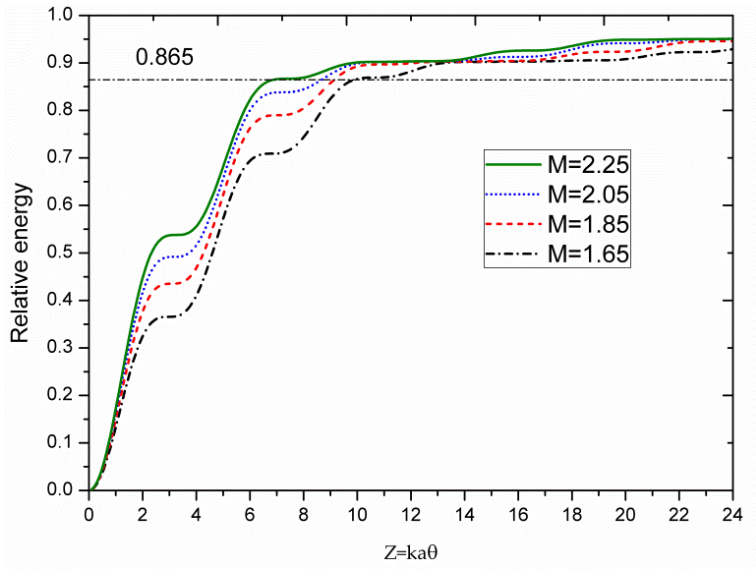

Figure 3. Angular distribution of the relative energy for different magnifications.

Table 2. Theoretical results of the divergence angle for the unstable resonator at different magnifications.

M	*Z*	*θ*/mrad
1.65	9.9	0.479
1.85	9.2	0.445
2.05	8.7	0.421
2.25	7.0	0.339

3. Experimental Arrangement

The experiments were performed using a pulsed DF laser with an active mixture SF_6:D_2 = 8:1 and with a total pressure of 9.5 kPa. The emission from this laser occupied the spectral range 3.6–4.2 μm with a center wavelength of 3.8 μm. Figure 4 presents the optical schematic of the experiments.

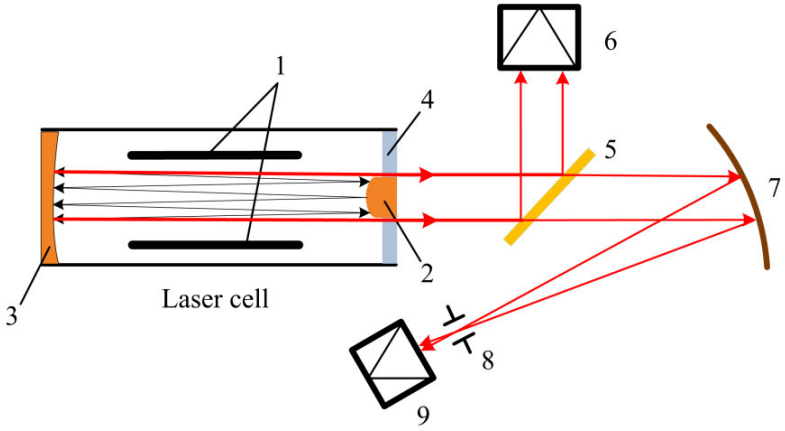

Figure 4. Scheme of the setup for measuring the far-field divergence of the laser beam: (1) electrodes; (2) convex mirror of the unstable resonator; (3) concave mirror; (4) output mirror; (5) plane-parallel plate beam splitter made of CaF_2; (6, 9) Gentec QE50LP-H-MB energy meter; (7) focusing mirror; and (8) aperture.

The discharge was formed between electrodes 1 of size 120 × 4 cm, which were spaced by a 4 cm gap. The discharge circuit was the same as that used in Ref. [2]. The positive-branch unstable resonator was formed from concave and convex spherical copper mirrors 2 and 3. The discharge chamber was sealed by the concave mirror 3 and output mirror 4. The convex mirror 2 was axially mounted on a full transparent output mirror 4 made of CaF_2, as shown in Figure 5. The convex mirror 2 was cooled by flow gas. Compared with the transverse support installation structure used in Ref. [30] and external cavity structure used in Refs. [25–27], the axial mounting inner cavity structure has the advantages of causing no obstruction to the laser beam, having no impact on the output power, causing no distortion in the output beam, being easy to adjust, and having a lower cost.

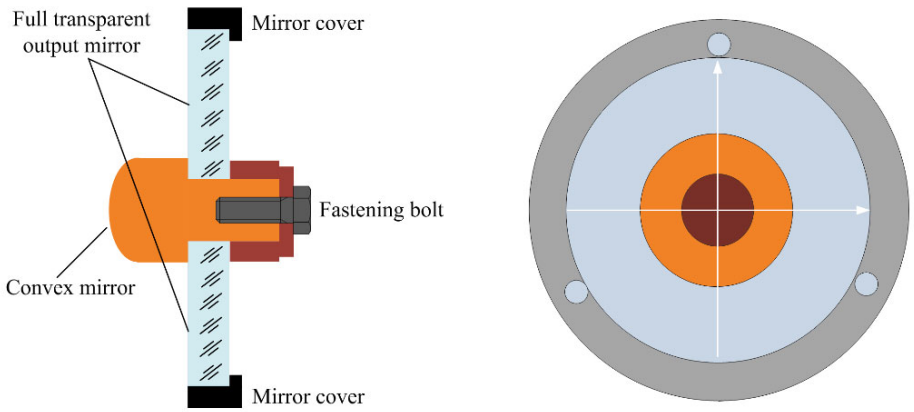

Figure 5. Installation structure diagram of the convex mirror.

The laser beam was divided into two beams by beam splitter 5; one entered the energy meter 6 to measure the near-field laser energy, and the other beam was focused by reflecting focusing mirror 7 to measure the divergence in the far-field zone. Energy meter 6 was replaced with heat-sensitive paper when recording the near field beam spot. The divergence measuring system consisted of a reflecting focusing mirror 7 with a focal length f = 10 m, a changeable calibrated aperture 8, which was placed in the focal plane of mirror 7, and an energy meter 9, which was placed behind the aperture 8. The distance between the laser exit and the reflecting focusing mirror was 5.5 m, and the angle between the incident

beam and the reflected beam on the reflecting focusing mirror was less than 22°. The beam divergence of the chemical laser was measured by the method of calibrated apertures.

A plane concave cavity formed by a totally concave reflecting copper mirror and a CaF_2 plate output mirror was used in the stable non-chain DF laser to compare the far-field beam performance between the unstable and stable resonators.

4. Experimental Results and Their Discussions

Based on the definition of far-field spot size with 86.5% surrounding energy, the far-field divergence angle θ can be written as $\theta = 2\ r/f$. Here r is radius of the circle containing 86.5% of the total energy, and f is the focal length of the focusing mirror. There are two different reference standards for the reference value of total laser energy in the focal plane: one with the aperture 8 fully opened (φ = 27.5 mm) and the other with the aperture 8 removed. Then, we gradually reduced the aperture size, measured the laser energy, and calculated the percentage compared with the reference value. We performed comparative measurements of radiation divergence for these two types at M = 1.65 and the results are presented in Figure 6.

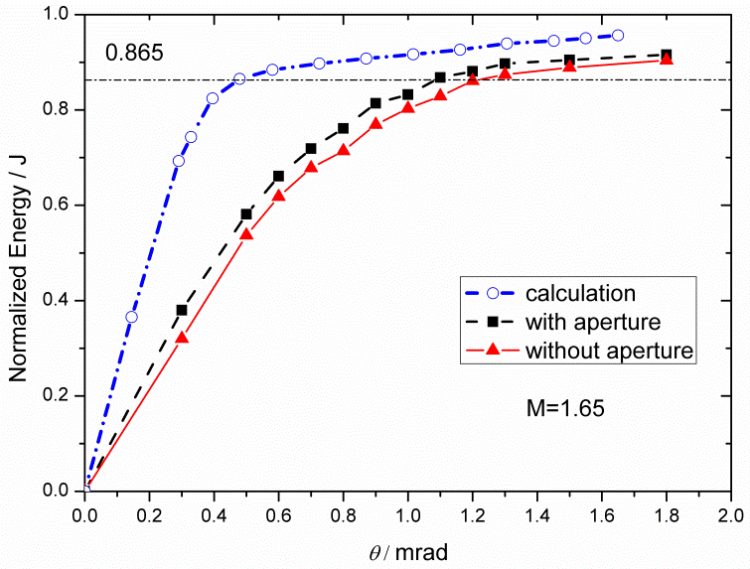

Figure 6. Normalized energy distribution of laser emission as a function of the angle embraced by the aperture.

Due to the existence of stray light in the cavity, the total energy of aperture fully opened was slightly lower than that without the aperture, and the difference was between 2% and 7%. Because of the large defecting angle, this stray light is ignored in far-field applications. In the following parts for M = 1.85, 2.05, and 2.25, we just consider the type with aperture fully opened when measuring the total energy. The far-field divergence angle for these two types at M = 1.65 was 1.08 and 1.19 mrad, respectively, and the energy distribution in the experiment was similar to that of the calculation. The maximum energy at 1 m distance from the laser exit was 2.76 J. Figure 7 shows the near-field spots at 1, 6, and 10 m distance from the laser exit and far-field spot at the focal plane recorded by the heat-sensitive paper and organic glass.

As we can see from Figure 7, the near-field spots had good symmetry in both the horizontal and vertical directions. The near-field spots had a round shape in the vertical direction and straight edges in the horizontal direction. The size of the ring-shaped near-field spot at 1 m was about 46.5 × 48.1 mm in the horizontal and vertical directions, and the radius of the center hole was about 30.2 mm, which was the same as the size of the convex mirror. The straight edges in the horizontal direction are caused by the interception of light beam by electrodes. The size of the back mirror of the unstable cavity was 50 mm, while

the distance between discharge electrodes was 40 mm, so light beams in the horizontal direction were partly cut by the electrode edges. A straight-edge diffraction appeared in the near-field spots at 1 m, which is also caused by the electrode diffraction at the edges. As the distance increased, the ring hole diffraction pattern became more obvious. Because the power intensity decreases with the propagation distance, the near field spot at 10 m had poor clarity compared with spots at 1 m and 6 m. The far-field ablation spot distribution on the heat-sensitive paper was relatively uniform at center, but the vertical size was larger than the horizontal size at the external circle. This can be eliminated by applying a back mirror with a diameter smaller than the electrode gap, which would decrease the total output energy. In practical applications, the energy and beam quality should be weighed according to the requirements of applications.

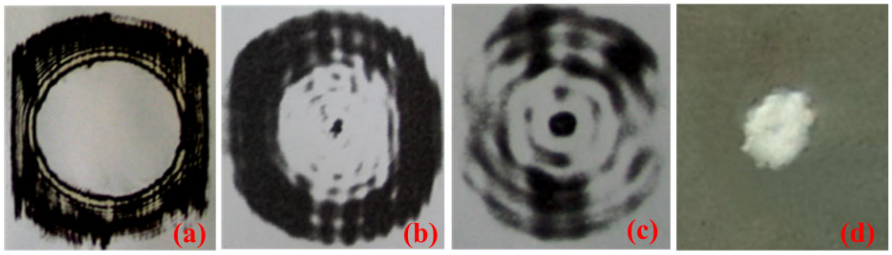

Figure 7. Laser spots at different places on the heat-sensitive paper: (**a**) 1 m; (**b**) 6 m; and (**c**) 10 m distance from the laser exit; and (**d**) far-field.

The beam divergence and output energy were compared between different magnifications under the same gas parameters, which were SF_6: D_2 = 8:1 and P_{total} = 9.5 kPa. Figure 8 shows the dependence of output energy on the charge voltage under different magnifications.

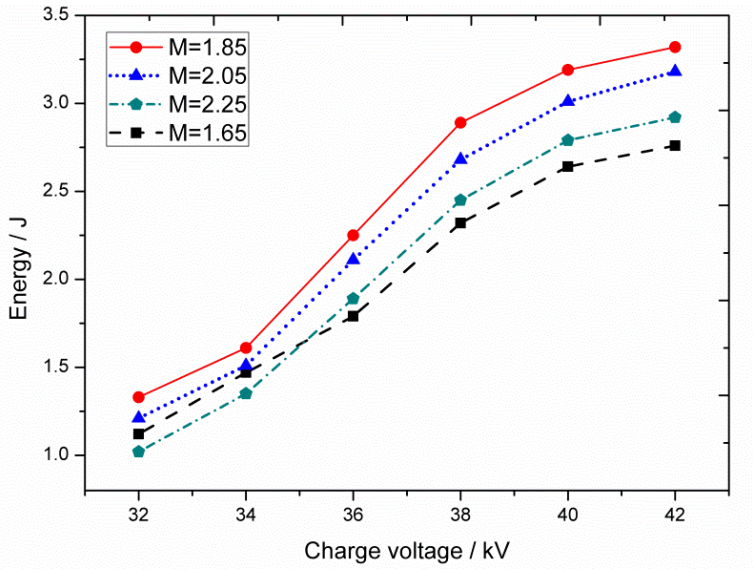

Figure 8. Laser energy versus charge voltage under different magnifications.

The output energy increases with the charge voltage, and the increase rate at lower voltages is larger than that at high voltages. As we know, for a certain gas pressure, there exists an optimum charge voltage for the active medium to be adequately excited. At lower voltages, too little excitation energy makes the generated excited state DF molecules too small, and thus the laser energy is low. As the charge voltage increases, the injection energy increases, resulting in a sharp increase in output energy. Once the charge voltage is greater than the optimal voltage corresponding to the optimal E/P value (where E is electric field

strength and P is pressure of the working mixture), arc discharge occurs and energy growth becomes slow. Severe arc discharge will greatly reduce the uniformity of discharge, thus reducing the laser energy and making damages on the electrodes. At each voltage, the energy does not have a linear relationship with M. As we can see from Table 1, the output coupling coefficient C increased with the magnification M, but the effective gain volume decreased with M. Therefore, there exists an optimum magnification to balance the gain volume and output coupling.

Figure 9 shows the near-field output energy and far-field energy density under different magnifications at charge voltage Uc = 42 kV. The far-field energy density was calculated by $\rho = E/S_f$, where E is the near-field output energy and S_f is the far-field spot area. Considering the application in remote atmospheric monitoring, the far-field operation range is >10 km. As we can see from Figure 9, the near field energy increased at first and then decreased, with a maximum energy E_{max} = 3.32 J attained at M = 1.85, while the far-field energy density increased monotonically.

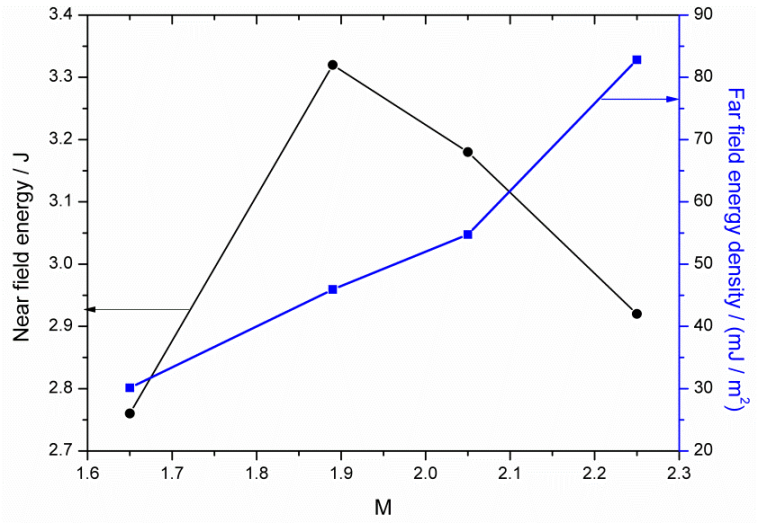

Figure 9. The dependence of near-field laser energy and far-field energy density on M.

Table 3 contains the results of divergence and energy values of our investigation. An increase in M reduced the divergence from θ = 1.08 mrad for M = 1.65 to 0.66 mrad for M = 2.25, and the corresponding diffraction limit factor $\beta = \theta_{exp}/\theta_{cal}$ reduced from 2.25 to 1.95. Further increasing the magnification could effectively reduce the laser divergence, but restricted by the size of the electrode gap in our present equipment, the size of the concave reflecting mirror should in the range 4~5 mm, and the corresponding size of the convex mirror should be <1.7cm for M > 3. The reduction of the size of the convex mirror would further increase the assembly difficulty of the resonator, which in turn may worsen the beam quality of the laser.

Table 3. Calculated and experimental results of the unstable non-chain DF laser.

Type	M	θ_{cal}/mrad	θ_{exp}/mrad	$\beta = \theta_{exp}/\theta_{cal}$	E/J	ρ/(mJ/m^2)
stable	—	0.190	7.15	37.63	3.65	0.91
unstable	1.65	0.479	1.08	2.25	2.76	30.1
unstable	1.85	0.445	0.97	2.18	3.32	45.9
unstable	2.05	0.421	0.86	2.04	3.18	54.7
unstable	2.25	0.339	0.66	1.95	2.93	82.8

The practical divergence angle of the unstable resonator in our investigation was relatively small, but it was still much larger than the theoretical value. The reasons are as follows:

(1) The light beam is regarded as a parallel light when calculating the theoretical divergence angle of the confocal unstable resonator. However, the actual output beam of the unstable resonator should be a near-parallel light with a certain geometric divergence angle, which is caused by factors such as cavity mirror spacing, curvature error, and mirror tilt;
(2) The straight-edge diffraction caused by electrode diffraction will also increase the actual divergence of the laser beam;
(3) The thermal denaturation of the output and convex mirrors increases the size of the divergence angle.

Although the unstable resonator had about 10–24% energy reduction in terms of overall output energy compared with the stable resonator, the measured beam quality and 10 km far-field energy density were much better, being increased by 11 and 91 times, respectively.

The laser beam and energy can be further improved by increasing the separation d between electrodes. For a given pressure of the working mixture, the charge voltage at optimum E/P would increase with d, and the resulting higher energy injection in the discharge chamber would lead to higher output energy for the DF laser. Meanwhile, the increase of d also allows a higher magnification M without increasing the difficulty of cavity adjustment. For example, when $d \geq 7$cm, a diameter $D_2 = 7$ of the concave mirror allows an M as high as 4.

5. Conclusions

A detailed investigation on the beam quality of a pulsed electric-discharged non-chain DF laser with a compact confocal positive-branch resonator was performed. The inner cavity with a convex mirror axially mounted on the output mirror was used. Four groups of unstable optical resonators with magnifications M = 1.65, 1.85, 2.05, and 2.25 were designed, and the intensity, energy distribution, and divergence angles were calculated. The experimental results of the divergence angles had a range of 1.08–0.66 mrad from M = 1.65 to M = 2.25, and the corresponding laser energy varied from 2.76 to 3.32 J, with the maximum energy achieved at M = 1.85. The far field energy density had a monotonic increase with M, and the maximum energy density was 82.8 mJ/m^2 at M = 2.25. The beam quality in the experiment was 2.25–1.95 times higher than in the calculation. The reasons for this difference were analyzed. In future research, we will eliminate the influence of electrode diffraction by properly selecting the size of the back mirror, reduce the thermal deformation of the output mirror by improving the refrigeration mode, and investigate the influence of mirror tilt on the beam quality.

Author Contributions: Investigation, C.S.; methodology, Q.P.; supervision, F.C. and J.G.; writing—original draft, L.Z.; writing—review and editing, P.R. All authors have read and agreed to the published version of the manuscript.

Funding: This study was supported by National Key R&D Program of China (2018YFE0203202), Natural Science Foundation of Jilin Province (20220101207JC), Science and technology cooperation project between Jilin Province and Chinese Academy of Sciences (2021SYHZ0028), State Key Laboratory of Laser Interaction with Matter Project (SKLLIM2115), Youth Innovation Promotion Association CAS (2021216).

Institutional Review Board Statement: Not applicable.

Informed Consent Statement: Not applicable.

Data Availability Statement: The data presented in this study are available on request from the corresponding author.

Conflicts of Interest: The authors declare no conflict of interest.

References

1. Belevtsev, A.A.; Firsov, K.N.; Kazantsev, S.Y.; Kononov, I.G.; Podlesnykh, S.V. Self-sustained volume discharge in mixtures of SF6 with hydrocarbons, hydrogen and deuterium for non-chain HF(DF) lasers. *J. Phys. D Appl. Phys. Europhys. J.* **2018**, *51*, 384003. [CrossRef]
2. Pan, Q.; Xie, J.; Wang, C.; Shao, C.; Shao, M.; Chen, F.; Guo, J. Non-chain pulsed DF laser with an average power of the order of 100 W. *Appl. Phys. B Lasers Opt.* **2016**, *122*, 200. [CrossRef]
3. Yang, N.; Li, G.; Zhao, Y.; Zhang, J.; Wen, X. Investigation on pulsed discharge mode in SF_6-C_2H_6 mixtures. *Plasma Sci. Technol.* **2020**, *22*, 109–116. [CrossRef]
4. Tao, M.; Shen, Y.; Zhu, F.; Huang, C.; Ma, L.; Chen, H.; Luan, K.; Huang, K.; Feng, G.; Ye, X. Pulse energy sustainability of a burst mode closed-cycle pulsed HF chemical laser. *Laser Phys.* **2019**, *29*, 35001. [CrossRef]
5. Driscoll, R.J.; Tregay, G.W. Flow field experiments on a DF chemical laser. *AIAA J.* **2015**, *21*, 241–246. [CrossRef]
6. Apollonov, V.V. High energy HF (DF) lasers. *J. Phys. Res. Appl.* **2018**, *1*, 1–16.
7. Apollonov, V.V.; Kazantsev, S.Y. High-Energy HF (DF) Lasers Based on Non-Chain Chemical Reaction. *J. Pure Appl. Phys.* **2020**, *2*, 1–13.
8. Altmann, J.; Pokrowsky, P. Sulfur dioxide absorption at DF laser wavelengths. *Appl. Opt.* **1980**, *19*, 3449–3452. [CrossRef] [PubMed]
9. Pokrowsky, P. Absorption of H_2S at DF laser wavelengths. *Appl. Opt.* **1983**, *22*, 2221–2223. [CrossRef]
10. Agroskin, V.Y.; Bravy, B.G.; Chernyshev, Y.A. Aerosol sounding with a lidar system based on a DF laser. *Appl. Phys. B* **2005**, *81*, 1149–1154. [CrossRef]
11. Vasilev, B.I.; Mannoun, O.M. IR differential-absorption lidars for ecological monitoring of the environment. *Quantum Electron.* **2006**, *36*, 801–820. [CrossRef]
12. Wilson, G.; Graves, B.R.; Patterson, S.P.; Wank, R.H. Deuterium fluoride laser technology and demonstrators. In Proceedings of the SPIE Laser Technologies for Defense and Security, Orlando, FL, USA, 10 September 2004; Volume 5414, pp. 41–51.
13. Ruan, P.; Pan, Q.; Alekseev, E.E.; Kazantsev, S.Y.; Mashkovtseva, L.S.; Mironov, Y.B.; Podlesnikh, S.V. Performance improvement of a Fe^{2+}:ZnSe laser pumped by non-chain pulsed HF laser. *Optik* **2021**, *242*, 167005. [CrossRef]
14. Velikanov, S.D.; Elutin, A.S.; Pegoev, I.N.; Sin'kov, S.N.; Frolov, Y.N. Measurement of the coefficients of reflection of DF laser radiation from topographic retroreflectors. *Quantum Electron.* **1998**, *28*, 173–174. [CrossRef]
15. Mirov, S.B.; Moskalev, I.S.; Vasilyev, S.; Smolski, V.; Fedorov, V.V.; Martyshkin, D.; Peppers, J.; Mirov, M.; Dergachev, A.; Gapontsev, V. Frontiers of mid-IR lasers based on transition metal doped chalcogenides. *IEEE J. Sel. Top. Quantum Electron.* **2018**, *24*, 1601829. [CrossRef]
16. Firsov, K.N.; Gavrishchuk, E.M.; Ikonnikov, V.B.; Kazantsev, S.Y.; Kononov, I.G.; Kotereva, T.V.; Savin, D.V.; Timofeeva, N.A. Room-temperature laser on a ZnSe:Fe^{2+} polycrystal with undoped faces, excited by an electrodischarge HF laser. *Laser Phys. Lett.* **2016**, *13*, 55002. [CrossRef]
17. Pan, Q.; Xie, J.; Chen, F.; Zhang, K.; Yu, D.; He, Y.; Sun, J. Transversal parasitic oscillation suppression in high gain pulsed Fe^{2+}:ZnSe laser at room temperature. *Opt. Laser Technol.* **2020**, *127*, 106151. [CrossRef]
18. Alekseev, E.E.; Kazantsev, S.Y.; Podlesnikh, S.V. Potential of crystals with a nonuniform doping profile for a Fe^{2+}:ZnSe laser. *Opt. Mater. Express* **2020**, *10*, 2075–2084. [CrossRef]
19. Apollonov, V.V.; Kazantsev, S.Y.; Saifulin, A.V.; Firsov, K.N. Discharge characteristics in a nonchain HF(DF) laser. *Quantum Electron.* **2000**, *30*, 483–485. [CrossRef]
20. Tarasenko, V.F.; Panchenko, A.N. Efficient discharge-pumped non-chain HF and DF lasers. In Proceedings of the SPIE Laser Beam Control and Applications, San Jose, CA, USA, 21–26 January 2006; Volume 6101, pp. 61011–61019.
21. Harris, M.R.; Morris, A.V.; Gorton, E.K. A closed-cycle, 1 kHz pulse repetition frequency, HF (DF) laser. In Proceedings of the SPIE Gas and Chemical Lasers and Intense Beam Applications, San Jose, CA, USA, 12 May 1998; Volume 3268, pp. 247–251.
22. Velikanov, S.D.; Evdokimov, P.A.; Zapol'Sky, A.F.; Kodola, B.E.; Sokolov, D.V.; Cernopyatov, V.Y.; Yakovlev, E.D. Pulse periodic HF (DF)-laser of atmospheric pressure with pulse repetition rate up to 2200 Hz. In Proceedings of the SPIE XVII International Symposium on Gas Flow, Chemical Lasers, and High-Power Lasers, Lisboa, Portugal, 17 April 2009; Volume 7131, pp. 228–234.
23. Aksenov, Y.N.; Borisov, V.P.; Burtsev, V.V.; Velikanov, S.D.; Voronov, S.L.V.; Voronin, V.V.; Zapol'skii, A.F.; Kirillov, G.A.; Kovalenko, O.I.; Lazarenko, V.I.; et al. A 400-W repetitively pulsed DF laser. *Quantum Electron.* **2001**, *31*, 290–292. [CrossRef]
24. Huang, C.; Huang, K.; Ma, L.; Zhu, F.; Yi, A.-P. Hundred-Hertz nonchain HF laser with long operation period based on initiated discharge. *Opt. Precis. Eng.* **2019**, *27*, 1060–1068. [CrossRef]
25. Bulaev, V.D.; Kulikov, V.V.; Petin, V.N.; Yugov, V.I. Experimental study of a nonchain HF laser on heavy hydrocarbons. *Quantum Electron.* **2001**, *31*, 218–220. [CrossRef]
26. Apollonov, V.V.; Belevtsev, A.A.; Firsov, K.N.; Kazantsev, S.Y.; Saifulin, A.V. Advanced studies on powerful wide-aperture non-chain HF(DF) lasers with a self-sustained volume discharge to initiate chemical reaction. In Proceedings of the SPIE XIV International Symposium on Gas Flow, Chemical Lasers, and High-Power Lasers, Wroclow, Poland, 10 November 2003; Volume 5120, pp. 529–541.
27. Brunet, H.; Mabru, M.; Voignier, F. High energy-high average power pulsed HF/DF chemical laser. In Proceedings of the SPIE Gas Flow and Chemical Lasers: Tenth International Symposium, Friedrichshafen, Germany, 31 March 1995; Volume 2502, pp. 388–392.

28. Rensch, D.B.; Chester, A.N. Iterative diffraction calculations of transverse mode distributions in confocal unstable laser resonators. *Appl Opt.* **1973**, *12*, 997–1010. [CrossRef] [PubMed]
29. Born, M.; Wolf, E. *Principles of Optics*, 6th ed.; Pergamon Press: Oxford, UK, 1980; pp. 416–418.
30. Tan, G.; Xie, J.; Pan, Q.; Shao, C.; Zhang, C.; Ruan, P.; Guo, J. Design and Experimental Investigation on Unstable Resonator for Non-Chain Pulsed DF Laser. *Chin. J. Lasers* **2014**, *41*, 102004.